

Nonlinear analysis of cable structures under general loadings



Mostafa Salehi Ahmad Abad, Ahmad Shooshtari*, Vahab Esmaeili, Alireza Naghavi Riabi

Faculty of Engineering, Ferdowsi University of Mashhad, Mashhad, Iran

ARTICLE INFO

Article history:

Received 1 January 2013

Accepted 1 May 2013

Keywords:

Static analysis

Cable structures

Geometric nonlinearity

Catenary cable

ABSTRACT

In this paper, two new elements for three-dimensional finite element analysis of cable structures are proposed. The tangent stiffness matrices of the cable elements are derived under spatially concentrated and distributed static and thermal loads. The first element, which is called Continuous Catenary Cable (CCC) element and extends the classic catenary cable element, presents the explicit forms of the stiffness matrix and internal force vector of the cable. The second element, Discrete Catenary Cable (DCC) element, is introduced by transforming the continuous equations of the CCC element into discrete formulation, giving the capability of dividing the cable into several straight elements with axial behavior. The DCC element, having all the features of the CCC element, has the advantages of including more three-dimensional loadings such as point loads along the member and non-uniform distributed lateral loads, and incorporating various geometrical and material nonlinearities such as cable cross-section variation and cable material yielding. Thereafter, employing the proposed elements, we have presented a simple algorithm for the analysis of pretensioned cables. The proposed elements are then used for nonlinear analysis of cable structures, and the response is compared with those obtained by other researchers. The results of numerical examples indicate the capability and robustness of the proposed elements in predicting the deformation response of cable structures.

© 2013 Elsevier B.V. All rights reserved.

1. Introduction

In recent decades, cable structures have been widely utilized in engineering applications due to their various advantages such as high strength, high degrees of flexibility, elastic behavior, light weight, the possibility of pretensioning and cost-effective construction [1]. Despite these advantages, high geometric nonlinearity has always been a potential threat to the stability of cable structures [2]. Because of this challenging problem, the analysis of these structural systems has attracted the attention of many researchers [3]. The proposed models are mainly classified into two categories including the models on the basis of finite element method and the classic elastic catenary expressions. From the first point of view, truss elements and multi-node curved elements, having both translational and rotational degrees of freedom, are presented [4]. The simplest element is truss element most commonly used in the analysis of cable structures [5–8], and has been resulted in a proper response for low-sag, highly stretched cables; in this case, the equivalent elastic modulus can be used to improve the accuracy [9]. The multi-node curved elements have been presented and extended as well [10–15]. Although using these elements results in more accurate responses [10,12], having no access to explicit form of

stiffness matrix and internal force vector may cause numerical and convergence problems [16].

Elastic catenary cable formulation, first presented by O'Brien and Francis [17] and later on extended by Andreu et al. [18] and Chunjiang et al. [19], is based on the equilibrium state of the cable element having only two nodes at its ends. This formulation, as compared to approximate finite element models, considers nonlinear effects accurately and requires less number of elements in cable structures modeling. Moreover, the use of the parabolic curve as an approximate geometry of a catenary cable is reportedly acceptable when cable experienced small curvatures [20–23]. Besides, the stiffness matrix is implicitly a function of the cable's internal forces and available in global coordinates. Recently, Thai and Kim [24], Impollonia et al. [25] and Salehi Ahmad Abad et al. [26] presented cable elements for nonlinear analysis of cable structures. Thai and Kim [24] precisely considered the effect of self-weight, and obtained the tangent stiffness matrix and internal force vector explicitly under static and dynamic loading. The effect of material nonlinearity lumped at the two ends of the elements was considered as well. Impollonia et al. [25] obtained the vector form of equilibrium equations as well as the closed form of the deformed shape; temperature variation, and uniformly distributed and point loads along the element have also been considered in their model. However, there is no access to explicit stiffness matrix and internal force vector. Salehi Ahmad Abad et al. [26] investigated the seismic response of cable structures and proposed a new catenary cable element for both material and geometric nonlinear dynamic analysis of these structures.

* Corresponding author. Tel.: +98 5118805105; fax: +98 5118763303.

E-mail addresses: ahmadshooshtari@yahoo.com,
ashoosht@ferdowsi.um.ac.ir (A. Shooshtari).

In this paper, the CCC element is proposed on the basis of the classic elastic catenary expressions; the explicit forms of the stiffness matrix and internal force vector of the cable are also available. Thereafter, with the use of the CCC model, the DCC element is proposed through transforming the continuous equations of the CCC element into discrete formulation; the DCC model provides the advantages of including more three-dimensional loadings such as point loads along the member and non-uniformly distributed lateral loads, and of incorporating various geometrical and material nonlinearities such as variation of the cable cross-section and yielding of the cable material. Then, a simple algorithm for the analysis of pretensioned cables is put forward with the use of our proposed elements. The results of the analysis of the cable structures using our proposed elements show that the DCC model analyses structures faster and with higher accuracy than continuous models.

2. Formulation

2.1. Continuous modeling

Herein, it is assumed that the cable is perfectly flexible, and is subjected to uniformly distributed and thermal loading along the member. The cross-sectional area of the element is kept constant as well. Fig. 1 shows the cable element under general loads. This element is suspended between points 1 and 2 with Cartesian coordinates (0, 0, 0) and (l₁, l₂, l₃), respectively. The uniformly distributed loads w₁, w₂ and w₃ are applied in global directions. Temperature variation is also considered. The Lagrangian coordinates of the un-deformed and deformed configurations are s and p. The equations for the equilibrium of the cable can be expressed as follows:

$$T \left(\frac{dx_1}{dp} \right) = -(w_1s + f_1) \tag{1a}$$

$$T \left(\frac{dx_2}{dp} \right) = -(w_2s + f_2) \tag{1b}$$

$$T \left(\frac{dx_3}{dp} \right) = -(w_3s + f_3) \tag{1c}$$

where f₁, f₂ and f₃ are the projected components of the cable force at the first node in x₁, x₂ and x₃ directions, respectively. The cable tension at the Lagrangian coordinates is given by

$$T(s) = \sqrt{\sum_{i=1}^3 (w_i s + f_i)^2} \tag{2}$$

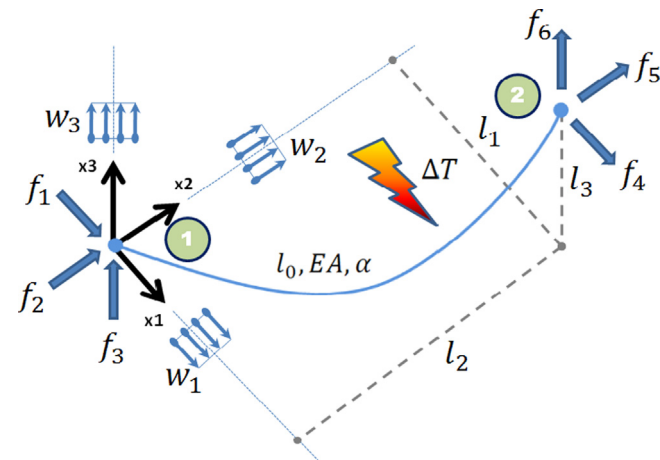


Fig. 1. Continuous model of catenary cable subjected to general loads.

The cable tension T is related to the strain ε by Hook's law as

$$T = EA(\epsilon - \epsilon_t) = EA \left(\frac{dp - ds}{ds} - \alpha \Delta T \right) = EA \left(\frac{dp}{ds} - 1 - \alpha \Delta T \right) \tag{3}$$

where EA, α and ΔT are the elastic modulus, cross-sectional area, linear thermal expansion coefficient of the materials, and the change in cable's temperature, respectively. The relationships between the Cartesian and Lagrangian coordinates are as follows:

$$x_i(s) = \int_0^s dx_i = \int_0^s \frac{dx_i dp}{dp ds} ds, \quad i = 1, 3 \tag{4}$$

Substituting Eqs. (1) and (3) into Eq. (4), we can find x_i as a function of s:

$$x_i(s) = \int_0^s \frac{-(w_i s + f_i)}{\sqrt{\sum_{i=1}^3 (w_i s + f_i)^2}} \left(\frac{\sqrt{\sum_{i=1}^3 (w_i s + f_i)^2}}{EA} + (1 + \alpha \Delta T) \right) ds, \tag{5}$$

i = 1, 3

The boundary conditions at the ends of the cable are

$$x_i(l_0) = l_i, \quad i = 1, 3 \tag{6a}$$

$$x_i(0) = 0, \quad i = 1, 3 \tag{6b}$$

where l₀ is the initial length of the cable element. By integrating along the member and applying the above boundary conditions, the projected lengths of the cable as functions of the internal forces, f_{i=1,3}, are derived as follows:

$$l_i(f_1, f_2, f_3) = -\frac{l_0 f_i}{EA} - \frac{l_0^2 w_i}{2EA} + \frac{1 + \alpha \Delta T}{w^3} \left(w w_i (T_1 - T_2) + (w^2 f_i - a_1 w_i) \left[\ln \left(\frac{a_1}{w} + T_1 \right) - \ln \left(t w + \frac{a_1}{w} + T_2 \right) \right] \right) \tag{7}$$

$w = \sqrt{\sum_{j=1}^3 w_j^2}, \quad a_1 = \sum_{j=1}^3 f_j w_j, \quad T_1 = T(0), \quad T_2 = T(l_0)$

In order to solve the above system of equations, differential projected components of the cable forces along x₁, x₂ and x₃ directions are required. These components are determined by

$$dl_i = \sum_{j=1}^3 \frac{\partial l_i}{\partial f_j} df_j \tag{8}$$

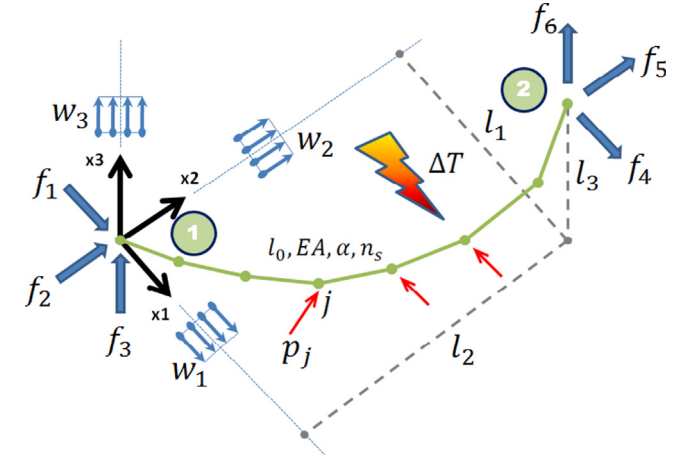


Fig. 2. Discrete model of catenary cable subjected to general loads.

In matrix form, Eq. (8) can be expressed as

$$\begin{Bmatrix} dl_1 \\ dl_2 \\ dl_3 \end{Bmatrix} = [F] \begin{Bmatrix} df_1 \\ df_2 \\ df_3 \end{Bmatrix} = \begin{bmatrix} \frac{\partial l_1}{\partial f_1} & \frac{\partial l_1}{\partial f_2} & \frac{\partial l_1}{\partial f_3} \\ \frac{\partial l_2}{\partial f_1} & \frac{\partial l_2}{\partial f_2} & \frac{\partial l_2}{\partial f_3} \\ \frac{\partial l_3}{\partial f_1} & \frac{\partial l_3}{\partial f_2} & \frac{\partial l_3}{\partial f_3} \end{bmatrix} \begin{Bmatrix} df_1 \\ df_2 \\ df_3 \end{Bmatrix} \quad (9)$$

where [F] is the flexibility matrix of the element. The general term of the flexibility matrix is given by

$$\frac{\partial l_i}{\partial f_j} = b_0(i,j) - \frac{1 + \alpha \Delta T}{w^3} [b_1(i,j) + b_2(i,j) \{ \ln(\frac{a_1}{w} + T_1) - \ln(\frac{a_1}{w} + T_2 + lw) \}] \quad (10)$$

the parameters are defined in

$$b_0(i,j) = \begin{cases} \frac{1}{EA}, & i=j \\ 0, & i \neq j \end{cases} \quad (11a)$$

$$b_1(i,j) = -ww_i \left[\frac{f_{j+3}}{T_2} + \frac{f_j}{T_1} \right] + (w^2 f_i - a_1 w_i) \left[\frac{w f_j + w_j (lw + T_2)}{T_2 (lw^2 + a_1 + w T_2)} - \frac{w f_j + w_j T_1}{T_1 (a_1 + w T_1)} \right] \quad (11b)$$

$$b_2(i,j) = \begin{cases} \frac{w_i^2 - w^2}{w_i w_j}, & i=j \\ \frac{w_i^2 - w^2}{w_i w_j}, & i \neq j \end{cases} \quad (11c)$$

The stiffness matrix is obtained by taking the inverse of the flexibility matrix as

$$[k] = [F]^{-1} \quad (12)$$

This stiffness matrix can be readily incorporated into the global tangent stiffness matrix of the CCC element with six degrees of freedom as

$$[K_T] = \begin{bmatrix} -k & k \\ k & -k \end{bmatrix} \quad (13)$$

The projected components of the internal forces at the second node of the element, i.e. f_4, f_5 and f_6 , are determined through the following equations of equilibrium:

$$f_4 = -(w_1 l_0 + f_1) \quad (14a)$$

$$f_5 = -(w_2 l_0 + f_2) \quad (14b)$$

$$f_6 = -(w_3 l_0 + f_3) \quad (14c)$$

where f_4, f_5 and f_6 are along x_1, x_2 and x_3 directions, respectively. Finally, the internal force vector is expressed as

$$\{F_{int}\} = \{f_1, f_2, f_3, f_4, f_5, f_6\}^T \quad (15)$$

2.2. Discrete modeling

Every cable member can be considered as a series of several truss elements. Therefore, by transforming Eq. (4) into a discrete form, a new discrete catenary cable (DCC) element is introduced. In this type of modeling, each cable member is divided into several truss elements allowing the concentrated loads to be applied along the element. Fig. 2 shows the DCC element and the associated applied loads.

The equations of equilibrium for the DCC element can be expressed as

$$T^j \left(\frac{\Delta x_i^j}{l^j} \right) = - \left(j l_s w_i + f_i + \sum_{k=1}^j p_i^k \right) \quad i = 1, 3, \quad j = 1, n \quad (16a)$$

$$\Delta x_i^j = x_i^{j+1} - x_i^j \quad (16b)$$

where n is the number of cable's sub-elements, j is the

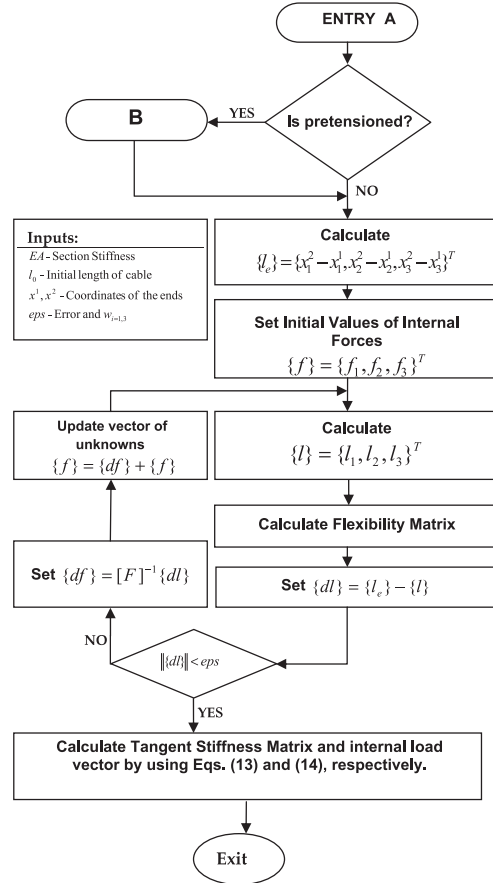


Fig. 3. Flow chart for computing internal forces and tangent stiffness matrix.

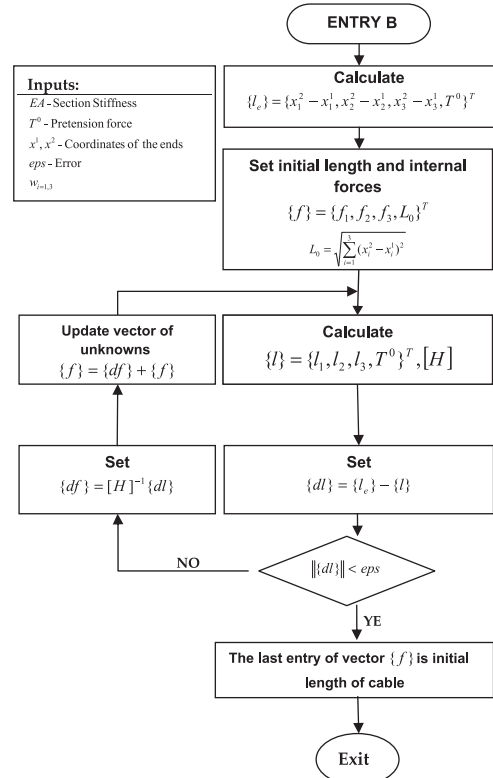


Fig. 4. Flow chart for computing internal forces and unstressed length for pretensioned cable.

sub-element's index, and i is the Cartesian coordinate in which the equilibrium condition is considered. l^j is the length of the j -th sub-element, and l_s is the unstressed length of each sub-element. p_i^k is the load applied to k -th internal node along i -direction. x_i^j is the component of the j -th sub-element in i -direction of the Cartesian coordinate system. T^j is the tension within the j -th sub-element and l_s is determined by

$$l_s = l_0/n \tag{17}$$

where l_0 is the unstressed length of the cable. The tension within each sub-element can be described as

$$T^j = \sqrt{\sum_{i=1}^3 \left(j l_s w_i + f_i + \sum_{k=1}^j p_i^k \right)^2}, \quad j = 1, n \tag{18}$$

According to Hook's law, the relationship between tension in each sub-element and strain is given by

$$T^j = E^j A^j \epsilon^j = E^j A^j \left(\frac{l^j - l_s}{l_s} - \alpha \Delta T \right) = E^j A^j \left(\frac{l^j}{l_s} - 1 - \alpha \Delta T \right) \tag{19}$$

where l^j is the deformed length of the j -th sub-element. The coordinates of the j -th node are calculated as

$$x_i^j = \sum_{k=1}^j \Delta x_i^k = \sum_{k=1}^j \frac{\Delta x_i^k}{l^k} l_s^k, \quad i = 1, 3 \tag{20}$$

by substituting Eqs. (16) and (19) into Eq. (20), and applying the boundary conditions, the following nonlinear system of equations with three unknowns will be achieved:

$$h_i(f_1, f_2, f_3) = -l_s \sum_{j=1}^n \left(j l_s w_i + f_i + \sum_{k=1}^j p_i^k \right) \left(\frac{1}{EA^j} + \frac{1 + \alpha \Delta T}{T^j} \right) \tag{21}$$

Table 1
Abbreviated names of the proposed elements.

Abbreviated name	Model
CCC	Continuous catenary cable
PCCC	Pretensioned continuous catenary cable
DCC	Discrete catenary cable
PDCC	Pretensioned discrete catenary cable
DCCWP	Discrete catenary cable with point loads

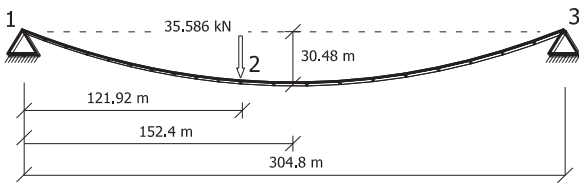


Fig. 5. Isolated cable under concentrated load.

Table 2
Initial properties of isolated cable under concentrated load.

Item	Data
Cross-sectional area	548.4 mm ²
Elastic modulus	131.0 kN/mm ²
Cable self-weight	46.12 N/m
Sag under self-weight at load point	29.276 m
Unstressed cable length of sections 1–2	125.88 m
Unstressed cable length of sections 2–3	186.85 m

Table 3
Comparison of displacements of isolated cable under concentrated load.

Researcher	Element type	Displacements (m)	
		Vertical	Horizontal
Michalos and Birnstiel [28]	Elastic straight	-5.472	-0.845
O'Brien and Francis [17]	Elastic catenary	-5.627	-0.860
Jayaraman and Knudson [29]	Elastic straight	-5.471	-0.845
Jayaraman and Knudson [29]	Elastic catenary	-5.626	-0.859
Tibert [4]	Elastic catenary	-5.626	-0.859
Andreu et al. [18]	Elastic catenary	-5.626	-0.860
Y. B. Yang and Tsay [30]	Elastic catenary	-5.625	-0.859
Thai and Kim [24]	Elastic catenary	-5.626	-0.859
Present work (DCC)	Elastic catenary	-5.592	-0.855
Present work (CCC)	Elastic catenary	-5.626	-0.859
Present work (DCCWP)	Elastic catenary	-5.830	-0.873

Taking the first derivative of Eq. (21) with respect to f_1, f_2 and f_3 , a matrix similar to Eq. (9) is obtained. The general term of the flexibility matrix is estimated by

$$\frac{\partial l_i}{\partial f_j} = \begin{cases} l_s \sum_{k=1}^n \left(\frac{1}{EA^k} + \frac{1 + \alpha \Delta T}{T^k} + \frac{(1 + \alpha \Delta T)(k l_s w_i + f_i + \sum_{n=1}^k p_i^n)^2}{(T^k)^3} \right), & i = j \\ l_s \sum_{k=1}^n \left(\frac{(1 + \alpha \Delta T)(k l_s w_i + f_i + \sum_{n=1}^k p_i^n)(k l_s w_j + f_j + \sum_{n=1}^k p_j^n)}{(T^k)^3} \right), & i \neq j \end{cases} \tag{22}$$

Ultimately, similar to the CCC element, the tangent stiffness matrix and the internal force vector of the DCC element can be evaluated with the use of Eqs. (13) and (15).

2.3. Application in pretensioned cable

In the case of pretensioned cables, the pretension force is known instead of the unstressed length. Therefore, four unknowns f_1, f_2, f_3 and l_0 , can be obtained by solving Eq. (23) simultaneously with Eqs. (7) or (21) for continuous and discrete conditions, respectively:

$$T^0 = \sqrt{\sum_{i=1}^3 f_i^2} \tag{23}$$

where T^0 is the pretension force of the cable. This system of equations can be solved by common iterative numerical methods such as Newton–Raphson. The Jacobian of the nonlinear system of equations is available through the following equation:

$$[H] = \begin{bmatrix} [F] & \left\{ \frac{\partial l}{\partial l_0} \right\}^T \\ \left\{ \frac{\partial T^0}{\partial f_i} \right\} & 0 \end{bmatrix} \tag{24a}$$

$$\left\{ \frac{\partial T^0}{\partial f_i} \right\} = \left\{ \frac{f_1}{T^0} \quad \frac{f_2}{T^0} \quad \frac{f_3}{T^0} \right\} \tag{24b}$$

$$\left\{ \frac{\partial l}{\partial l_0} \right\} = \left\{ \frac{\partial l_1}{\partial l_0} \quad \frac{\partial l_2}{\partial l_0} \quad \frac{\partial l_3}{\partial l_0} \right\} \tag{24c}$$

Matrix $[F]$ can be determined for the CCC and DCC elements using Eqs. (10) and (22), respectively. The components of vector $\left\{ \frac{\partial l_i}{\partial l_0} \right\}$ can also be computed using Eq. (25a) for the CCC element or Eq. (25b) for the DCC element:

$$\frac{\partial l_i}{\partial l_0} = - \left(\frac{1 + \alpha \Delta T}{T_2} + \frac{l_0}{EA} \right) f_{i+3}, \quad i = 1, 3 \tag{25a}$$

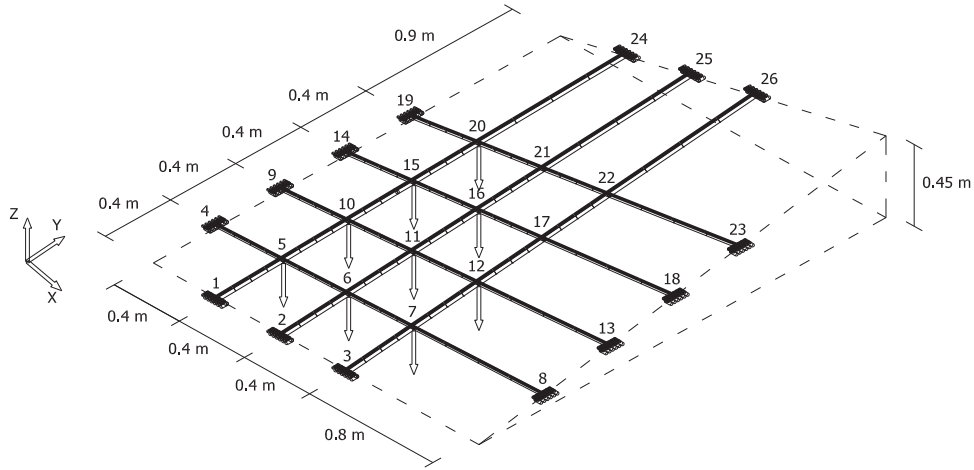


Fig. 6. Hyperbolic paraboloid net.

Table 4
Comparison of vertical displacements (mm) of hyperbolic paraboloid net.

Node	Experiment [31]	Dynamic relaxation [31]		Minimum Energy [32]		Elastic catenary [24]		Present work ^a (PDCC)		Present work ^b (PDCC)		Present work ^a (PCCC)		Present work ^b (PCCC)	
		Value	Error (%)	Value	Error (%)	Value	Error (%)	Value	Error (%)	Value	Error (%)	Value	Error (%)	Value	Error (%)
5	-19.50	-19.30	-1.03	-19.30	-1.03	-19.56	0.31	-19.51	-0.05	-19.99	-19.50	0.00	-19.92	-19.50	0.00
6	-25.30	-25.30	0.00	-25.50	0.79	-25.70	1.58	-25.57	1.07	-28.17	-25.56	1.03	-28.01	-25.56	1.03
7	-22.80	-23.00	0.88	-23.10	1.32	-23.37	2.50	-23.27	2.06	-27.47	-23.27	2.06	-27.24	-23.27	2.06
10	-25.40	-25.90	1.97	-25.80	1.57	-25.91	2.01	-25.82	1.65	-28.60	-25.81	1.61	-28.46	-25.81	1.61
11	-33.60	-33.80	0.60	-34.00	1.19	-34.16	1.67	-33.94	1.01	-40.93	-33.93	0.98	-40.63	-33.93	0.98
12	-28.80	-29.40	2.08	-29.40	2.08	-29.60	2.78	-29.42	2.15	-38.81	-29.41	2.12	-38.34	-29.41	2.12
15	-25.20	-26.40	4.76	-25.70	1.98	-25.86	2.62	-25.61	1.63	-30.66	-25.60	1.59	-30.44	-25.60	1.59
16	-30.60	-31.70	3.59	-31.20	1.96	-31.43	2.71	-31.01	1.34	-42.12	-31.00	1.31	-41.63	-31.00	1.31
17	-21.00	-21.90	4.29	-21.10	0.48	-21.56	2.67	-21.24	1.14	-35.28	-21.22	1.05	-34.53	-21.22	1.05
20	-21.00	-21.90	4.29	-21.10	0.48	-21.57	2.71	-20.84	-0.76	-27.42	-20.83	-0.81	-27.07	-20.83	-0.81
21	-19.80	-20.50	3.54	-19.90	0.51	-20.14	1.72	-19.20	-3.03	-32.73	-19.18	-3.13	-31.95	-19.18	-3.13
22	-14.20	-14.80	4.23	-14.30	0.70	-14.55	2.46	-13.83	-2.61	-30.33	-13.81	-2.75	-29.18	-13.81	-2.75
Error			10.6		4.5		7.8		6.0			6.1			6.1

^a $w_g = -0.195$ N/m, $w_x = w_y = 0$.
^b $w_g = -0.195$ N/m, $w_x = w_y = 30$ N/m.

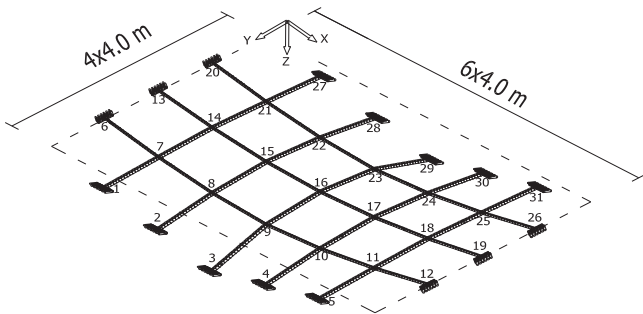


Fig. 7. Spatial net.

$$\frac{\partial l_i}{\partial l_0} = \frac{1}{n} \sum_{j=1}^n \frac{(1 + \alpha \Delta T)}{T^j} \left[T_i^j \left(1 - \frac{c_j j l_s}{(T^j)^2} \right) - j l_s w_i \right] - \frac{T_i^j + j l_s w_i}{(EA)^j}, \quad i = 1, 3$$

$$T_i^j = j l_s w_i + f_i + \sum_{k=1}^j p_i^k, \quad c_j = \sum_{k=1}^3 w_k T_k^j \quad (25b)$$

2.4. Verification of the proposed elements

In the previous sections, equations of elastic catenary cable element under general loads like uniformly distributed, 3D point

loads and thermal forces were derived. By assuming that the cable element is only exposed to self-weight ($w_1 = w_2 = 0, w_3 = -w_0$) and neglecting changes in temperature, the cable's projected length can be expressed as follows according to Eq. (7):

$$l_1 = -\frac{l_0 f_1}{EA} - \frac{f_1}{w_0} [\ln(T_2 + f_6) - \ln(T_1 - f_3)] \quad (26a)$$

$$l_2 = -\frac{l_0 f_2}{EA} - \frac{f_2}{w_0} [\ln(T_2 + f_6) - \ln(T_1 - f_3)] \quad (26b)$$

$$l_3 = -\frac{l_0 f_3}{EA} + \frac{w_0 l_0^2}{2EA} + \frac{1}{w_0} [T_2 - T_1] \quad (26c)$$

where T_1 and T_2 are the cable tensions at points 1 and 2, respectively. Also by applying the above-mentioned assumptions to Eq. (10) and simplifying the equations, the differential of the cable's projected lengths with respect to the internal forces can be computed as follows:

$$\frac{\partial l_1}{\partial f_1} = -\left(\frac{l_0}{EA} + \frac{1}{w_0} \ln \left[\frac{T_2 + f_6}{T_1 - f_3} \right] \right) + \frac{f_1^2}{w_0} \left[\frac{1}{T_1(T_1 - f_3)} - \frac{1}{T_2(T_2 + f_6)} \right]$$

$$\frac{\partial l_1}{\partial f_2} = \frac{\partial l_2}{\partial f_1} = \frac{f_1 f_2}{w_0} \left[\frac{1}{T_1(T_1 - f_3)} - \frac{1}{T_2(T_2 + f_6)} \right], \quad \frac{\partial l_1}{\partial f_3} = \frac{\partial l_3}{\partial f_1} = \frac{f_1}{w_0} \left[\frac{1}{T_2} - \frac{1}{T_1} \right]$$

Table 5
Comparison of displacements (mm) of spatial net.

Node	z-coord	Lewis et al. [31]			Thai and Kim [24]			Present work (PDCC)			Present work (PCCC)		
		dx	dy	dz	dx	dy	dz	dx	dy	dz	dx	dy	dz
1	1000.0	-	-	-	-	-	-	-	-	-	-	-	-
2	2000.0	-	-	-	-	-	-	-	-	-	-	-	-
3	3000.0	-	-	-	-	-	-	-	-	-	-	-	-
6	0	-	-	-	-	-	-	-	-	-	-	-	-
7	819.5	-5.14	0.42	30.41	-5.03	0.41	29.86	-5.05	0.40	29.55	-5.02	0.41	29.55
8	1409.6	-2.26	0.47	17.70	-2.23	0.46	17.29	-2.23	0.40	17.16	-2.24	0.43	17.55
9	1676.9	0.00	-2.27	-3.62	0.00	-2.31	-3.61	0.00	-2.36	-3.19	0.00	-2.33	-3.19
13	0	-	-	-	-	-	-	-	-	-	-	-	-
14	687.0	-4.98	0.00	43.49	-4.92	0.00	42.85	-4.93	0.00	42.94	-4.94	0.00	42.99
15	1147.8	-2.55	0.00	44.47	-2.55	0.00	44.26	-2.55	0.00	44.34	-2.56	0.00	44.30
16	1317.6	0.00	0.00	41.65	0.00	0.00	42.08	0.00	0.00	42.14	0.00	0.00	42.04

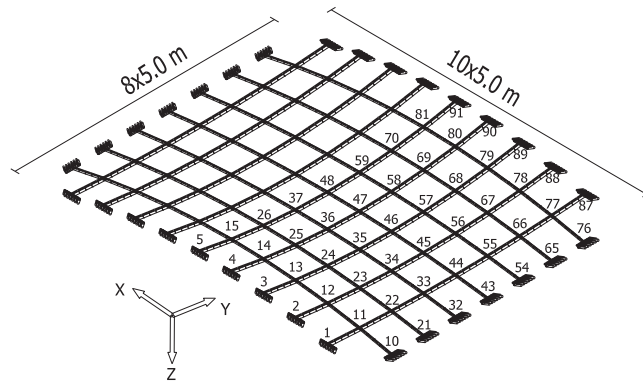


Fig. 8. Saddle net.

Table 6
Comparison of displacements (mm) of saddle net.

Node	z-coord	Kwan [3]			Thai and Kim [24]			Present work (PDCC)			Present work (PCCC)		
		dx	dy	dz	dx	dy	dz	dx	dy	dz	dx	dy	dz
1	-1368	-	-	-	-	-	-	-	-	-	-	-	-
2	-2432	-	-	-	-	-	-	-	-	-	-	-	-
3	-3192	-	-	-	-	-	-	-	-	-	-	-	-
4	-3648	-	-	-	-	-	-	-	-	-	-	-	-
5	-3800	-	-	-	-	-	-	-	-	-	-	-	-
11	-1032	15.55	-4.46	81.70	15.55	-4.46	81.66	15.58	-4.47	81.87	15.57	-4.46	81.79
12	-1835	11.50	-5.55	61.22	11.50	-5.54	61.18	11.52	-5.56	61.36	11.51	-5.55	61.28
13	-2408	7.38	-4.20	33.31	7.38	-4.19	33.28	7.39	-4.20	33.41	7.39	-4.20	33.36
14	-2752	5.34	-3.11	17.88	5.34	-3.11	17.87	5.34	-3.12	17.97	5.34	-3.11	17.92
15	-2867	4.11	-2.80	11.16	4.10	-2.80	11.15	4.10	-2.80	11.24	4.10	-2.80	11.21
22	-792	14.43	-3.53	97.14	14.42	-3.53	97.10	14.46	-3.54	97.44	14.44	-3.53	97.29
23	-1408	11.27	-4.47	72.90	11.26	-4.46	72.84	11.29	-4.48	73.17	11.28	-4.47	73.03
24	-1848	7.25	-2.97	31.98	7.25	-2.97	31.94	7.26	-2.98	32.2	7.25	-2.98	32.09
25	-2118	5.67	-2.12	10.54	5.67	-2.11	10.52	5.67	-2.13	10.74	5.67	-2.12	10.64
26	-2200	4.77	-0.60	-11.34	4.77	-0.60	-11.34	4.77	-0.61	-11.13	4.77	-0.60	-11.22
33	-648	11.71	-1.71	92.44	11.7	-1.71	92.40	11.74	-1.72	92.8	11.72	-1.71	92.63
34	-1152	9.55	-2.11	66.94	9.54	-2.11	66.89	9.57	-2.12	67.31	9.56	-2.11	67.13
35	-1512	6.30	-1.15	20.21	6.30	-1.15	20.17	6.31	-1.16	20.53	6.31	-1.16	20.37
36	-1728	4.92	-0.23	-14.05	4.91	-0.23	-14.06	4.92	-0.23	-13.74	4.92	-0.23	-13.88
37	-1800	4.65	0.52	-35.79	4.65	0.52	-35.77	4.64	0.52	-35.46	4.65	0.52	-35.59
44	-600	10.63	0.00	88.73	10.62	0	88.68	10.66	0	89.11	10.64	0	88.93
45	-1067	8.80	0	62.83	8.79	0	62.77	8.82	0	63.23	8.81	0	63.04
46	-1400	5.83	0	13.99	5.83	0	13.95	5.84	0	14.35	5.84	0	14.18
47	-1600	4.64	0	-22.52	4.63	0	-22.52	4.64	0	-22.17	4.64	0	-22.32
48	-1667	4.55	0	-45.89	4.54	0	-45.87	4.54	0	-45.51	4.54	0	-45.66
52	-600	-0.92	0	5.86	-0.92	0	5.86	-0.96	0	6.27	-0.94	0	6.10
72	-1848	3.85	-0.78	-30.12	3.85	-0.78	-30.10	3.83	-0.76	-29.82	3.84	-0.77	-29.94
81	-2867	4.11	2.80	11.16	4.10	2.80	11.15	4.10	2.80	11.24	4.10	2.80	11.21
85	-1032	-5.40	1.87	32.17	-5.40	1.87	32.15	-5.44	1.88	32.38	-5.42	1.88	32.28

$$\frac{\partial l_2}{\partial f_2} = -\left(\frac{l_0}{EA} + \frac{1}{w_0} \ln \left[\frac{T_2 + f_6}{T_1 - f_3} \right] \right) + \frac{f_2^2}{w_0} \left[\frac{1}{T_1(T_1 - f_3)} - \frac{1}{T_2(T_2 + f_6)} \right]$$

$$\frac{\partial l_2}{\partial f_3} = \frac{\partial l_3}{\partial f_2} = \frac{f_2}{w_0} \left[\frac{1}{T_2} - \frac{1}{T_1} \right], \quad \frac{\partial l_3}{\partial f_3} = -\frac{l_0}{EA} - \frac{1}{w_0} \left[\frac{f_6}{T_2} - \frac{f_1}{T_1} \right] \quad (27)$$

Table 7
Comparison of time of analysis of saddle net.

Element type	No. of segments	Time (s)	Maximum error (%)
PCCC	NA	37.42	–
PDCC	3	30.07	0.026
PDCC	5	31.84	0.021
PDCC	10	31.57	0.018
PDCC	15	31.26	0.017
PDCC	30	31.62	0.016
PDCC	75	31.70	0.016

Table 8
Initial properties of elastic cable subjected to a temperature rise $\Delta T=100$ K.

Item	Data
Cross-sectional area	1 m ²
Elastic modulus	3.0e7 N/mm ²
Cable self-weight	1 N/m
Thermal expansion coefficient	6.5e-6 1/K
Unstressed cable length	100 m

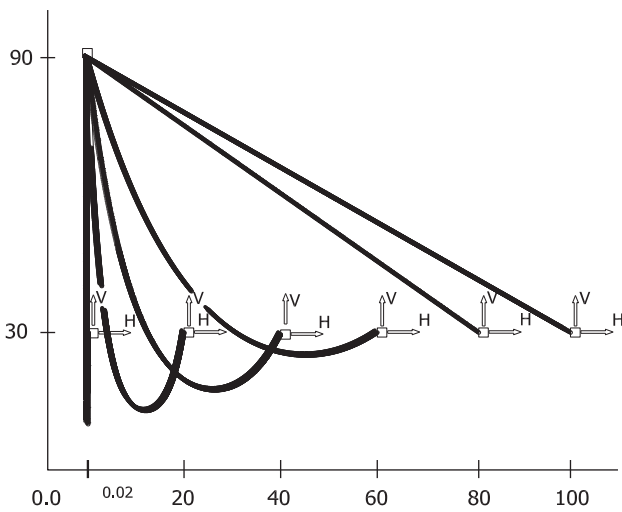


Fig. 9. Various configurations and end forces of the cable (m).

Table 9
Comparison of reaction forces (N) of elastic cable subjected to a temperature rise $\Delta T=100$ K.

Researchers	Pevrot and Goulois [33]		Yang and Tsay [30]		Present study (DCC)		Present study (CCC)	
	Reactions		Reactions		Reactions		Reactions	
Location (m)	H	V	H	V	H	V	H	V
0.02	0.00	20.02	0.01	20.02	0.010	19.99	0.011	20.02
20	3.061	19.93	3.061	19.93	3.090	19.83	3.060	19.93
40	9.172	19.24	9.172	19.24	9.16	19.14	9.172	19.24
60	22.15	15.73	22.15	15.73	22.11	15.63	22.145	15.73
80	504.0	-328	504.1	-328.9	504.48	-329.40	504.1037	-328.86
100	4 170 000	-2 511 000	4 255 700	-255 340	4 255 849	-2 555 047	4 258 491	-2 555 044

It is noteworthy that Eqs. (26) and (27) are reported by Thai and Kim [24] as well.

3. Stiffness matrix and internal force vector

In the proposed elements, the explicit form of the stiffness matrix and the internal force vector are available. Figs. 3 and 4 illustrate the process of deriving the stiffness matrix and internal force vector for a cable with a specific initial length or pretension force. Since there is no explicit solution for the determination of internal forces, the nonlinear system of equations must be solved in an iterative procedure such as Newton–Raphson method with quadratic convergence.

4. Numerical examples

According to the above discussions, in order to check the accuracy and capability of the present models, the necessary codes were developed in finite element package OpenSees [27]. Various examples for evaluating proposed models are discussed. The abbreviated names of the used models are presented in Table 1. For the pretensioned cable, a very small quantity is considered as the weight per unit length of the cable.

Example 1. An isolated cable spanning between two supports of 304.8 m distance at the same elevation is subjected to a concentrated load of 35.586 kN as shown in Fig. 5, where the sag at the mid-span is 30.48 m. The other required data are summarized in Table 2. The CCC, DCC and DCCWP elements are employed to solve this problem. Two CCC elements, two DCC elements and one DCCWP element are used for modeling this structure.

The externally concentrated loads are considered as internal forces for the DCCWP element. In the discrete model, each cable member is divided into five parts of the same length. Table 3 shows the comparison of the displacements related to the second node generated with the use of the proposed elements and other researchers. A good agreement can be seen between the results obtained by using the DCC elements and those predicted by continuous models, reflecting the point that this element can be used to analyze a cable with a low curvature.

Example 2. The pretensioned cable net, shown in Fig. 6, was experimentally and numerically investigated by Lewis et al. [31]; they used dynamic relaxation method to analyze this structure. Sufian and Templeman [32] also analyzed this structure with the use of the minimum energy method. Thai and Kim [24] calculated the cable's displacements through using the catenary cable model and Newton–Raphson procedure. This structure, as illustrated in Fig. 6, includes 31 cable elements with elastic behavior. Moreover,

some nodes of this structure are subjected to concentrated loads of 15.7 N, in the negative direction of z -axis. The cable's elastic modulus and cross-sectional area are respectively 128.3 kN/mm² and 0.785 mm². The cables, before being subjected to external loads, had been pretensioned under the force of 200 N. In order to analyze this structure, the PCCC and PDCC models have been applied. In the PDCC model, the cables were divided into four parts of the same length. To investigate the effects of the laterally distributed loads, the structure was subjected to a lateral load of 30 N/m in the X and Y directions. The results of the above-mentioned analysis and the errors with respect to the experimental values are shown in Table 4.

Example 3. Another example here is a spatial cable net including 4×4 quadrilaterals formed by 38 pretensioned cable segments, and being 16×24 in plan (Fig. 7). It has central symmetry, and the z -coordinate (z -coord) of the nodes of a quarter of the structure is shown in Table 5. The cables parallel to x - and y -direction have been pretensioned by forces of 90 kN and 30 kN, respectively. The vertically concentrated loads applied to all the internal nodes of this structure are 6.8 kN. The cables' cross-sectional areas in x - and y -direction are respectively 350 mm² and 120 mm². The elastic modulus of all the cables is considered to be 160 kN/mm². The cables using the PDCC element are divided into 10 parts. In Table 5, our measured displacements using the suggested models have been compared to the findings of Lewis et al. [31], and Thai and Kim [24].

Example 4. The cable net in Fig. 8 includes 142 pretensioned cable elements. The distances of the cables from each other are 5 m in both horizontal directions. The structure has central symmetry and vertical coordinates (z -coord) for a quarter of the structure presented in Table 6. All cables have the same pretension force of 60 kN. All cables using PDCC element are divided into 10 parts of the same length. The cables' cross-sectional area is 306 mm² and their modulus of elasticity is 147 kN/mm². Free nodes of half of this saddle net, are subjected to 1 kN external load in x - and z -directions.

Table 6 shows the comparison between nodal displacements generated by suggested models and the findings of Kwan [3] and Thai and Kim [24].

To compare the capability and efficiency of the discrete catenary cable and continuous models, the time consumed for each analysis and errors in both models are presented in Table 7; the results show that using the PDCC elements decreases the time required for the analysis up to 15% with an acceptable error.

Example 5. The cable, with an increasing temperature up to 100 °K, holds the characteristics mentioned in Table 8. The left end of the cable is fixed at the coordinates (0, 90), and the right end maintains a constant vertical elevation of 30 m, and the horizontal coordinate of the right end changes between 0 and 100 m, (Fig. 9). This case was analyzed by Pevrot and Goulois [33] and Yang and Tsay [30]. To solve this problem, they made use of the CCC and DCC elements. In all conditions, we use 30 parts of the same length for the PDCC element; but for the case that the horizontal space between the cable nodes is 0.02 m, in order to converge to answers, 650 elements were used. Our obtained results are presented in Table 9, comparing the capabilities of different elements.

5. Conclusion

In this research, a novel formulation for spatial catenary cable element was proposed. Two types of cable elements, continuous and discrete, were discussed. The models were found to be

applicable for general loads such as uniformly distributed, three-dimensional point, and thermal loads. Furthermore, the equations were modified for pretensioned cables. It should be pointed out that all necessary equations for practical analysis were presented here in the form of closed equations. The tangent stiffness matrix and corresponding internal force vector for both models were also presented. Necessary algorithms for calculating the stiffness matrix and the internal force vector for cables with/without pretensioning effect were presented as well.

The acceptable convergence of the proposed models, their simplicity and direct equations reflect their capability, found through making comparison with other models, in analyzing some given numerical examples. Moreover, the numerical examples showed that both continuous and discrete models provided good accuracy, while the latter was faster and reduced the time consumed for analysis up to 15% for large cable structures within acceptable errors.

References

- [1] G.D. Stefanou, Dynamic response of tension cable structures due to wind loads, *Comput. Struct.* 43 (1992) 365–372.
- [2] L. Liao, B. Du, Finite element analysis of cable-truss structures, in: 51st AIAA/ASME/ASCE/AHS/ASC Structures, Structural Dynamics, and Materials Conference, Orlando, Florida, USA, 2010.
- [3] A.S.K. Kwan, A new approach to geometric nonlinearity of cable structures, *Comput. Struct.* 67 (1998) 243–252.
- [4] G. Tibert, Numerical Analyses of Cable Roof Structures, KTH, 1999.
- [5] J.H. Argyris, D.W. Scharpf, Large deflection analysis of prestressed networks, *J. Struct. Div.* 98 (1972) 633–654.
- [6] M.L. Gambhir, B. Batchelor, Finite element study of the free vibration of 3-D cable networks, *Int. J. Solid. Struct.* 15 (1979) 127–136.
- [7] W.C. Knudson, Static and Dynamic Analysis of Cable-Net Structures, University of California, Berkeley, 1971.
- [8] H. Ozdemir, A finite element approach for cable problems, *Int. J. Solid Struct.* 15 (1979) 427–437.
- [9] H.J. Ernst, E. Der, Der e-modul von seilen unter beruecksichtigung des durchhanges, *Der Bauing.* 40 (1965) 52–55.
- [10] H.M. Ali, A.M. Abdel-Ghaffar, Modeling the nonlinear seismic behavior of cable-stayed bridges with passive control bearings, *Comput. Struct.* 54 (1995) 461–492.
- [11] J.P. Coyette, P. Guisset, Cable network analysis by a nonlinear programming technique, *Eng. Struct.* 10 (1988) 41–46.
- [12] M.L. Gambhir, B. Batchelor, A finite element for 3-D prestressed cablenets, *Int. J. Numer. Meth. Eng.* 11 (1977) 1699–1718.
- [13] T. Jianmin, S. Zuyan, Q. Ruojun, A nonlinear finite element method with five-node curved element for analysis of cable structures, in: Proceedings of IASS International Symposium, 1995, pp. 929–935.
- [14] J.Y.R. Liew, N.M. Punniyakotly, N.E. Shanmugam, Limit-state analysis and design of cable-tensioned structures, *Int. J. Space Struct.* 16 (2001) 95–110.
- [15] Z.H. Chen, Y.J. Wu, Y. Yin, C. Shan, Formulation and application of multi-node sliding cable element for the analysis of Suspen-Dome structures, *Finite Elem. Anal. Des.* 46 (2010) 743–750.
- [16] M. Yang, Z. Chen, X.G. Hua, A new two-node catenary cable element for the geometrically non-linear analysis of cable-supported structures, *Proc. IME C J. Mech. Eng. Sci.* 224 (2010) 1173–1183.
- [17] W.T. O'Brien, A.J. Francis, Cable movements under two-dimensional loads, *J. Struct. Div. ASCE* 90 (1964) 89–124.
- [18] A. Andreu, L. Gil, P. Roca, A new deformable catenary element for the analysis of cable net structures, *Comput. Struct.* 84 (2006) 1882–1890.
- [19] W. Chunjiang, W. Rengeng, D. Shilin, Q. Ruojun, A new catenary cable element, *Int. J. Space Struct.* 18 (2003) 269–275.
- [20] M.G. Huang, W.X. Ren, A new parabolic cable element in static analysis, in: The Ninth International Conference on Inspection, Appraisal, Repairs and Maintenance of Structures, Fuzhou, China, 2005, pp. 271–282.
- [21] J.H. Wu, W.Z. Su, The non-linear finite element analysis of cable structures based on four-node isoparametric curved element, *J. Chongqing Jianzhu Univ.* 27 (2005) 55–58 (in Chinese).
- [22] M. Yang, Z. Chen, Nonlinear analysis of cable structures using a two-node curved cable element of high precision, *Eng. Mech.* 20 (2003) 42–47 (in Chinese).
- [23] S. Ren, M. Gu, Static analysis of cables' configuration in cable-stayed bridges, *J. Tongji Univ.* 33 (2005) 595–599, in Chinese.
- [24] H.T. Thai, S.E. Kim, Nonlinear static and dynamic analysis of cable structures, *Finite Elem. Anal. Des.* 47 (2011) 237–246.
- [25] N. Impollonia, G. Ricciardi, F. Saitta, Statics of elastic cables under 3D point forces, *Int. J. Solid Struct.* 48 (2011) 1268–1276.
- [26] M. Salehi Ahmad Abad, A. Shoostari, V. Esmaeili, A. Naghavi Riabi, Material and geometric nonlinear dynamic analysis of cable structures under seismic excitations, in: 15th World Conference on Earthquake Engineering, Lisbon, Portugal, 2012.

- [27] F. McKenna, G.L. Fenves, M.H. Scott, et al., Open System for Earthquake Engineering Simulation, University of California, Berkeley, CA, 2000.
- [28] J. Michalos, C. Birnstiel, Movements of a cable due to changes in loading, *Trans. Am. Soc. Civ. Eng.* 127 (1962) 267–281.
- [29] H.B. Jayaraman, W.C. Knudson, A curved element for the analysis of cable structures, *Comput. Struct.* 14 (1981) 325–333.
- [30] Y.B. Yang, J.Y. Tsay, Geometric nonlinear analysis of cable structures with a two-node cable element by generalized displacement control method, *Int. J. Struct. Stab. Dyn.* 7 (2007) 571–588.
- [31] W.J. Lewis, M.S. Jones, K.R. Rushton, Dynamic relaxation analysis of the non-linear static response of pretensioned cable roofs, *Comput. Struct.* 18 (1984) 989–997.
- [32] F.M.A. Sufian, A. Templeman, On the non-linear analysis of pre-tensioned cable net structures, *Struct. Eng.* 4 (1992) 147–158.
- [33] A.H. Pevrot, A.M. Goulois, Analysis of cable structures, *Comput. Struct.* 10 (1979) 805–813.